APPLIED ORGANOMETALLIC CHEMISTRY
Appl. Organometal. Chem. **14**, 831–835 (2000)

Active phase of iron catalyst for alcohol formation in hydrogenation of carbon oxides†

Hisanori Ando,* Yasuyuki Matsumura and Yoshie Souma
Osaka National Research Institute, AIST, Midorigaoka, Ikeda, Osaka 563-8577, Japan

Hydrogenation of CO_2 over iron catalysts has been carried out and compared with the activity obtained with CO. The rates of hydrocarbon and alcohol formation were higher in the reaction with CO. The rates of hydrocarbon and alcohol formation were suppressed by addition of steam to the reactant gas mixture of H_2–CO_x. Although no significant change in the structure of the catalyst was observed by the X-ray diffraction analyses, change in the oxidation state of the surface iron was detected by recording X-ray photoelectron spectroscopy of the catalysts. During the reaction with CO, the catalyst surface was further reduced even after the reduction at 500 °C, whereas it was oxidized in the reaction with CO_2. A change in product distribution and the results of X-ray photoelectron spectroscopy analyses showed that the iron carbide is the active site for hydrocarbon formation and the oxygen species in iron hydroxide (O_{Fe}—OH) may be relevant to the formation of MeOH. Copyright © 2000 John Wiley & Sons, Ltd.

Keywords: carbon monoxide; carbon dioxide; hydrogenation; comparative study; alcohol; iron catalyst; XRD; XPS

1 INTRODUCTION

The transformation of CO_2 into useful chemicals such as hydrocarbons is an option for reduction of CO_2. Since iron-based catalysts have been widely used in the water-gas shift (WGS) reaction[1] as well as Fischer–Tropsch (F–T) reaction,[2–9] iron is a candidate as a catalyst for the hydrogenation of CO_2. However, the hydrogenation of CO_2 over iron catalyst is difficult for practical use at present because of its much lower reactivity than CO.[10–13] In addition H_2O produced by the reverse water-gas shift (RWGS) reaction may lead to deactivation of the iron catalyst. Hence, consideration of the differences in the catalyst surface affected by H_2O in the reaction with CO and CO_2 are necessary in order to develop new catalysts for CO_2 hydrogenation.

It is known that F–T synthesis over iron catalyst produces both hydrocarbons and oxygenates. The active phase for hydrocarbon formation is believed to be FeC_x. Miller and Moskovits showed a different pathway for oxygenate formation and this implies the presence of other active phases.[14] However, identification of the active phases is not easy because the surface iron is not stable during the reaction. That is, formation of FeC_x species accompanies accumulation of carbon on the surface and reduction of Fe_2O_3 to Fe_3O_4 and to metallic iron also proceeds.[6]

In the present study we have carried out the hydrogenation of CO and CO_2 over iron catalyst and compared the catalytic activities and the differences in the surface phase. We have also carried out the addition of steam into the reactant gas mixture to examine the effect of H_2O on the catalytic activity, as well as to clarify the change in the surface phase of the catalyst.

2 EXPERIMENTAL

Iron catalyst was prepared by calcination of iron hydroxide in air at 500 °C for 3 h. The resulting solid was crushed into <60 mesh granules by using a mortar. The hydrogenation of CO_x was carried out with a fixed-bed flow reactor made of stainless steel tube with 10 mm i.d. The catalyst was pretreated

* Correspondence to: H. Ando, Osaka National Research Institute, AIST, Midorigaoka, Ikeda, Osaka 563-8577, Japan.
E-mail: h-ando@onri.go.jp
† This paper is based on work presented at the Fifth International Conference on Carbon Dioxide Utilization (ICCDU V), held on 5–10 September 1999 at Karlsruhe, Germany.

Table 1 Hydrogenation of CO_x over iron catalyst (rate of formation; unit: μmol h^{-1} per gram of catalyst)

Reactant (composition)	CO_x	Hydrocarbons		Alcohols			Selectivity to alcohols[a]
		C_{1-4}	C_{5+}	MeOH	EtOH	PrOH	
H_2/CO (67/33)	20.3	69.3	52.8	22.4	11.6	4.5	24
H_2/CO_2 (75/25)	3.3	7.5	1.0	1.6	0.3	0	12
$H_2/CO/H_2O$ (42/21/37)	20.1	1.1	0.5	1.9	0.2	0	56
$H_2/CO_2/H_2O$ (48/16/36)	0	<0.1	0	0.1	0	0	95[b]

Conditions: 250 °C, 1 MPa, stable activity.
[a] (Yields of C_{1-3} alcohols)/(total yield − yield of CO_x) ×100.
[b] The CO_2 conversion was 0.1%.

with a diluted hydrogen (10 vol% H_2 in N_2) stream (50 ml min^{-1}) under atmospheric pressure at 500 °C for 1 h. After sufficient cooling of the reactor, the reactant gas mixture (33 vol% CO in H_2 or 25 vol% CO_2 in H_2) was introduced and, pressure was raised to 1 MPa and temperature was set at 250 °C. The effluent gas was analyzed with on-line gas chromatographs the columns of which were Porapak Q for CO_2, MS-13X for methane and CO, PLOT (fused silica, Al_2O_3/KCl) for hydrocarbons, and PEG-6000(15%) + TCEP(8%) supported on Chromosorb WAW(60/80 mesh) for alcohols. Yields and selectivities were calculated on the basis of carbon numbers in the products.

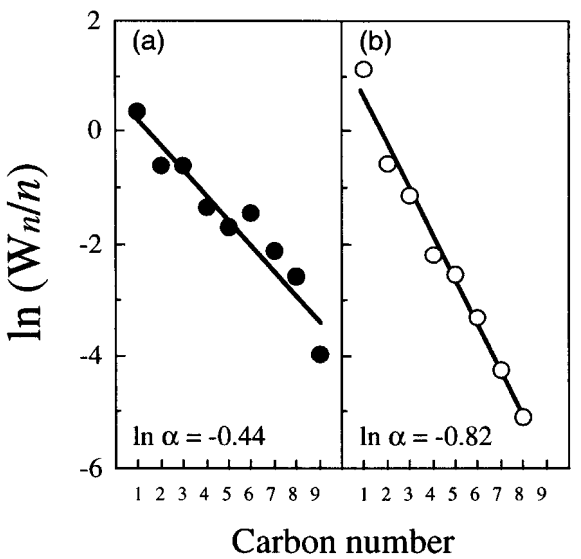

Figure 1 Schulz–Flory plots for the hydrogenation over iron catalyst reduced at 500 °C: (a) reaction with CO; (b) reaction with CO_2.

The BET surface areas of the catalysts were determined from the isotherms of nitrogen physisorption. X-ray diffraction (XRD) patterns were recorded with a Rigaku ROTAFLEX diffractometer (Cu Kα, 40 kV, 150 mA). Surface analyses by X-ray photoelectron spectroscopy (XPS) were performed with a Shimadzu ESCA-750. The spectra were recorded after argon-ion etching for 1 min (2 kV, 25 mA). The binding energy was corrected with the energy of C(1*s*) (284.6 eV) for carbon contaminant.[15]

3. RESULTS AND DISCUSSION

3.1 Catalytic performance of iron catalyst

The catalytic hydrogenation of CO_x over iron catalyst reduced at 500 °C is summarized in Table 1. Since the purpose of this study is not to develop a highly active catalyst but to elucidate the factor that controls the catalytic performance in the reaction with CO_x, the reaction conditions described in Table 1 were not optimized to get good yield. In the reaction with CO, the major products were C_1–C_9 hydrocarbons, C_1–C_3 alcohols, and CO_2. The product distribution of hydrocarbons almost obeyed the Schulz–Flory law (Fig. 1a). From the plots of the carbon number n vs $\ln(W_n/n)$, the probability of chain growth α was estimated as 0.64. When CO_2 is used as a reactant, C_1–C_5 hydrocarbons, C_1 and C_2 alcohols, and CO were obtained. The distribution of hydrocarbons produced also obeyed the Schulz–Flory law (Fig. 1b), showing that the hydrogenation of CO_2 proceeds along with the F–T-type reaction scheme followed by the RWGS reaction. A smaller value of α for CO_2 hydrogenation (0.44)

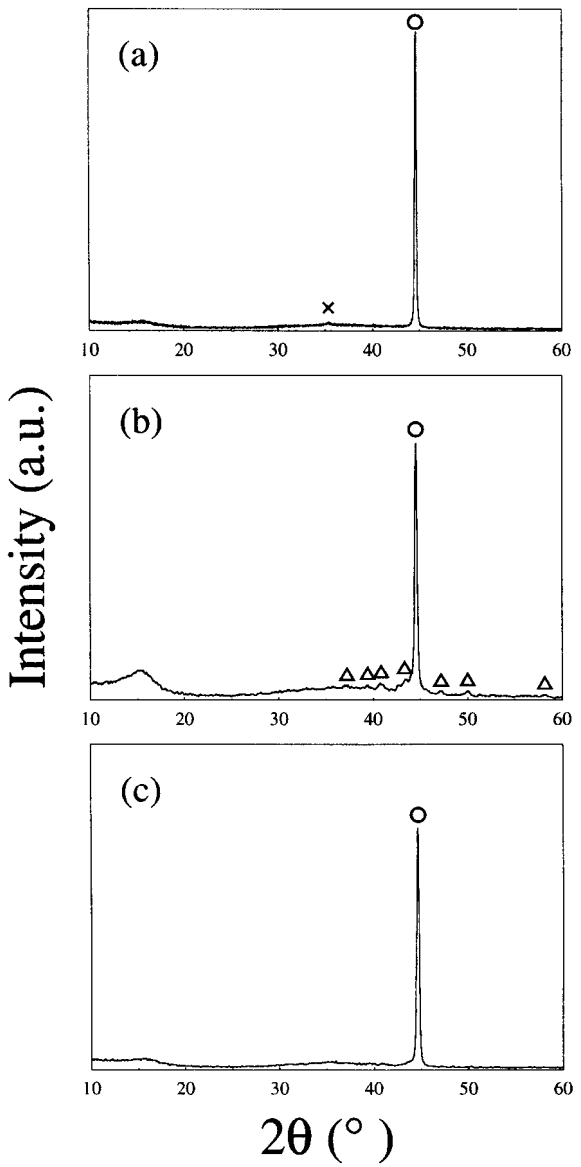

Figure 2 XRD patterns for iron catalysts, (○) Fe, (×) Fe_3O_4, (△) $Fe_{2.2}C$: (a) after reduction at 500 °C; (b) followed by reaction with CO; (c) followed by reaction with CO_2.

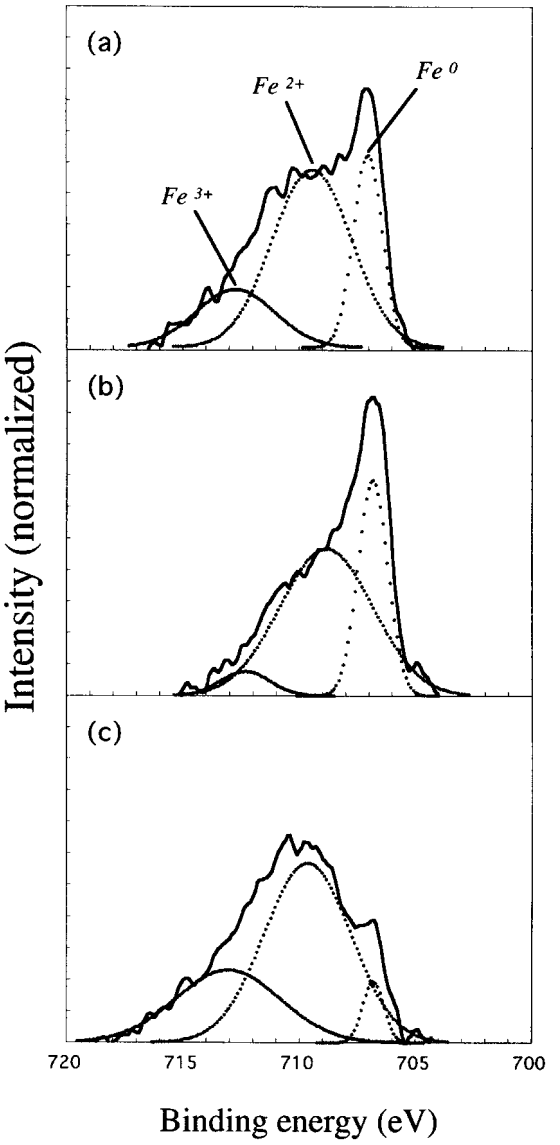

Figure 3 XPS spectra of Fe($2p_{3/2}$) for iron catalysts: (a) after reduction at 500 °C; (b) followed by reaction with CO; (c) followed by reaction with CO_2.

than that obtained in the CO reaction reflects the higher selectivity to light hydrocarbons (see Table 1).

It is noteworthy that the formation rate of CO_2 was almost the same before and after addition of H_2O. The rates of hydrocarbon and alcohol formation were suppressed by addition of H_2O, then totally, the selectivity to alcohols increased (see Table 1). This means that the site for hydrocarbon formation was deactivated. It is conceivable that H_2O oxidizes the surface iron and this may prevent formation of carbide species. The catalyst seems to have the activity for MeOH formation even after addition of H_2O, whereas the rates for C_{2+} alcohol production almost diminished (see Table 1), suggesting that the site for C_{2+} alcohol formation is relevant to that for hydrocarbon formation.

Table 2 Surface analysis by XPS for iron catalysts

Reactant	Surface composition (mol%)					[Fe]/[O][a]
	Fe^0	Fe^{2+}	Fe^{3+}	O_{Fe-OH}	O_{Fe-O}	
—[b]	13	32	10	16	29	1.2
H_2/CO	19	40	3	17	21	1.6
H_2/CO_2	2	28	14	23	33	0.8
$H_2/CO/H_2O$	0	18	18	40	24	0.6
$H_2/CO_2/H_2O$	0	16	18	42	24	0.5

Conditions: Mg Kα, 8 kV, 30 mA. Ar^+ etching (2 kV, 25 mA) for 60 s was performed before measurement.
[a] [Fe], total amount of Fe species; [O], total amount of O species.
[b] After reduction with H_2/N_2.

On the other hand, the catalytic activity almost disappeared when H_2O was added to CO_2 hydrogenation. Only trace amounts of methane and methanol were observed. The apparent selectivity to alcohols was high owing to low conversion of CO_2.

3.2 Characterization of iron catalyst

When the reaction finished, the reactant gas was switched to helium gas and the reactor was cooled to room temperature. The sample was taken out from the reactor and transferred into XRD or XPS instruments in air. Reymond *et al.*[6] confirmed that the exposure of samples composed of iron to air is not a serious drawback for the reliability of the characterization of the catalyst,[6,16] however, the reason why is as yet unclear.

XRD analyses showed a clear peak attributed to α-Fe at 44.6 ° in 2θ for the sample taken out from the reactor just after the reduction at 500 °C (Fig. 2a). The sample taken out from the reactor after the reaction with CO retained the structure, and peaks attributed to χ-$Fe_{2.2}C$ were also recorded (Fig. 2b). The sample after the reaction with CO_2 also kept the α-Fe structure but no peaks attributed to carbide species were observed (Fig. 2c). This implies that the presence of CO_2 in the reactant can prevent the formation of carbide species, which is considered as an intermediate in the F–T reaction.

Although no significant change in the structure of the catalyst except for formation of carbide species during the hydrogenation of CO was observed by the XRD analyses, a change in the oxidation state of the surface iron was detected by XPS of the catalysts. In the range of Fe($2p_{3/2}$) a major peak attributed to Fe^0 was recorded by XPS at 706.7 eV for the catalyst just after the reduction at 500 °C.[15] The spectrum can be deconvoluted to three Gaussian peaks and minor peaks were at 709.3 and 712.5 eV after the reaction with CO (Fig. 3a). The former can be attributed to Fe^{2+} and the latter to Fe^{3+}.[15] No peak or shoulder attributed to iron carbide was observed. The profiles for O(1*s*) were also separated into two Gaussian peaks at 529.5 and 531.1 eV; the former can be attributed to the oxygen connecting to iron and the latter to the oxygen in the hydroxide (O_{Fe-OH}).[15]

The surface compositions were calculated by using the atomic sensitivity factors for each element.[15] and they are tabulated in Table 2. The value of the [Fe]/[O] ratio just after the pretreatment was 1.2 and those after the reaction with CO and CO_2 were 1.6 and 0.8 respectively. The amount of metallic iron increased and the χ-$Fe_{2.2}C$ phase was detected by XRD for the sample after the reaction with CO, showing that the iron carbide is an active species for hydrocarbon formation. Although no metallic iron phase was observed in the sample after addition of steam, the selectivity to alcohol increased. This implies the presence of other active phases to produce alcohols. On the other hand, the surface iron was oxidized after the reaction with CO_2 and this may prevent formation of carbide species, resulting in low hydrocarbon formation.

In the reaction with $H_2/CO/H_2O$, the suppression of the rate of MeOH formation was not so significant, whereas those of C_{2+} alcohol formation were drastically suppressed (see Table 1). This means that the active site for MeOH formation is different from those for C_{2+} alcohol. Furthermore, the amount of O_{Fe-OH} species increased by addition of steam (see Table 2), suggesting that the O_{Fe-OH} species plays an important role in the formation of MeOH; however, further investigation is necessary to clarify the details.

REFERENCES

1. Newsome DS. *Catal. Rev. Sci. Eng.*, 1980; **21**(2): 275.
2. Soled S, Iglesia E, Fiato RA. *Catal. Lett.* 1990; **7**: 271.
3. Bukur DB, Mukesh D, Patel SA. *Ind. Eng. Chem. Res.* 1990; **29**: 194.
4. Dictor RA, Bell AT. *J. Catal.* 1986; **97**: 121.
5. Dry ME. In *Catalysis Science and Technology*, vol. 1, Anderson JR, Boudart M (eds.). Springer: New York, 1982; 159.
6. Reymond JP, Mériaudeau P, Teichner SJ. *J. Catal.* 1982; **75**: 39.
7. Blanchard F, Reymond JP, Pommier B, Teichner SJ. *J. Mol. Catal.* 1982; **17**: 171.
8. Madon RJ, Taylor WF. *J. Catal.* 1981; **16**: 32.
9. Raupp GB, Delgass WN. *J. Catal.* 1979; **58**: 361.
10. Dwyer DJ, Somorjai GA. *J. Catal.* 1978; **52**: 291.
11. Lee J-F, Chern W-S, Lee M-D, Dong T-Y. *Can. J. Chem. Eng.* 1992; **70**: 511.
12. Lee M-D, Lee J-F, Chang C-S. *Bull. Chem. Soc. Jpn.* 1989; **62**: 2756.
13. Pijolat M, Perrichon V, Primet M, Bussiére P. *J. Mol. Catal.* 1982; **17**: 367.
14. Miller D, Moskovits M. *J. Am. Chem. Soc.* 1989; **111**: 9250.
15. Wagner CD, Riggs WM, Davis LE, Moulder JF. In *Handbook of X-ray photoelectron spectroscopy*, Muilenberg GE. (ed.). Perkin–Elmer Corp: Minnesota, 1978.
16. Amelse JA, Butt JB, Schwartz LH. *J. Phys. Chem.* 1980; **84**: 3363.